



Sharif University of Technology  
Scientia Iranica  
Transactions A: Civil Engineering  
<http://scientiairanica.sharif.edu>



## Analytical approach to evaluate stability of pile-stabilized slope

M. Hajiazizi<sup>a</sup>, A. Mazaheri<sup>b</sup>, and R.P. Orense<sup>c,\*</sup>

a. Department of Civil Engineering, Razi University, Kermanshah, Iran.

b. Department of Civil Engineering, University of Ayatollah ozma Boroujerdi, Boroujerd, Iran.

c. Department of Civil & Environmental Engineering, University of Auckland, Auckland, New Zealand.

Received 9 November 2016; received in revised form 1 February 2017; accepted 11 March 2017

### KEYWORDS

Slope stability;  
Pile;  
Safety factor;  
Stability analysis;  
Arching.

**Abstract.** Many studies have been conducted to examine the factor of safety of a slope reinforced by a row of piles and the forces acting on these piles. This paper presents an analytical approach to calculate the forces acting on piles and the corresponding factor of safety of slopes stabilized by a row of piles. The proposed approach is based on force equilibrium within the upslope wedge above the pile location and would require knowledge of the upper wedge weight before application. The validity of the proposed analytical approach was verified by comparing the results with those obtained using available approaches in the literature as well as from physical experiments and numerical analyses using available software. Additionally, the effect of arching phenomenon was examined and the optimum pile spacing for use in reinforcing slopes was investigated. The optimum pile spacing depends on the properties of the soil comprising the slope, but the most cost-effective pile spacing was found to be between 4-5 times the pile diameter, corresponding to the largest spacing that could generate arching between piles. Thus, the proposed analytical approach can be used in practical applications to determine the stability of slopes reinforced by a row of piles.

© 2018 Sharif University of Technology. All rights reserved.

### 1. Introduction

One of the most effective strategies for stabilizing slopes undergoing creep movement and for increasing the stability of soil slopes is pile reinforcement [1]. cursory review of available literature shows that slope stabilization using piles has been analysed by various researchers using different methods [2-6]. These methods can be divided into three categories: (1) shear strength reduction method [7,8]; (2) limit equilibrium

methods [9-12]; and (3) limit analysis method based on upper bound and lower bound theories [13-16].

In the stabilization of earth slopes by using piles, the general approach is to determine the minimum factor of safety,  $F_S$ , to make it stable (e.g.,  $F_S \geq 1.5$ ) and to calculate the design load on the pile from the applied forces and moments [17]. Numerical analysis results have shown that the best location to install the stabilizing piles is at the middle of the portion of the slope defined by the critical sliding surface [6,7,18-20]. For example, Poulos [3] suggested that the piles be installed at the middle of the failure wedge to prevent the creation of the sliding surfaces in both upstream and downstream of the piles.

Ito et al. [2] proposed a method based on limit equilibrium to evaluate the stability of slope reinforced

\*. Corresponding author. Tel.: + 64 9 373 7599;  
Fax: + 64 9 373 7462  
E-mail address: [r.orense@auckland.ac.nz](mailto:r.orense@auckland.ac.nz) (R.P. Orense)

by piles, and obtained the lateral force acting on the piles caused by soil mass movement based on the theoretical equations developed by Ito and Matsui [21]. In this method, the force acting on the piles depends on soil properties, overburden pressure, and lateral spacing between the piles [1]. It is worthy to mention that the equation presented by Ito and Matsui [21] is valid only for a specific range of spacing between the piles and therefore, it is not appropriate to use for large or even very small spacing [22]. In applying this method, it is assumed that the soil around the piles is deformable and limitation on the length of the piles as well as soil arching between the piles can be neglected [22,23]. Hassiotis et al. [10] proposed an extension of this method to determine the force acting on a single row of piles using plasticity theory.

Lee et al. [24] proposed a method to analyse the response of the piles using limit equilibrium analysis, where the piles were considered as a simple beam and the soil was considered as a continuous elastic model. The method calculates the shear force acting on each pile, as well as pile lateral displacement. Moreover, Li et al. [25] studied the seismic displacement of soil slopes reinforced by piles and they proposed a seismic yield coefficient using the upper bound method and calculated the force acting on the piles by using Ito and Matsui [21] equation. Kourkoulis et al. [22] presented a hybrid method to design piles by calculating the force on the piles based on Broms' equation [26] and determined the characteristics of the pile accordingly. Kourkoulis et al. [22] suggested dimensionless design charts based on reinforced concrete piles embedded in rock, which were produced for a specific example to illustrate the effectiveness of the proposed method in practice. Furthermore, they examined arching between piles and the length of embedded pile in dense layer. Kahyaoglu et al. [27] examined the effect of the spacing between the piles and pile head fixity, and the distribution of the forces behind the pile using laboratory studies and image processing.

Although various methods have been proposed to determine the forces acting on the piles, they generally lack the required accuracy, especially for both very small and large pile spacing; in addition, some of the methods require parameters which are difficult to obtain in conventional practice.

In this paper, a new equation is proposed to calculate the force acting on the stabilizing pile, considering the failure surface, the lateral forces exerted by the weight of the failure wedge, and 3 soil resistance characteristics. The formulation also allows the calculation of the factor of safety of the reinforced slope. Pile displacement can be computed using elastic beam theory. Aside from solid theoretical background, the proposed approach is very convenient to use and provides good agreement with the results of other

methods available in the literature. The approach is also validated by comparing the results with those obtained using PLAXIS software. Thus, the proposed analytical method is more practical and could be easily used by geotechnical engineers.

## 2. Proposed analytical approach

The proposed analytical approach for determining the force acting on piles is based on the weight of upslope wedge. For this purpose, two sliding block stability analyses are formulated: (1) the force acting on piles in two-dimensional case; and (2) its extension to three-dimensional condition.

### 2.1. Two-dimensional formulation

As mentioned earlier, limit equilibrium method is one of the concepts used by various researchers to investigate the force acting on the piles reinforcing the soil slope. A general view of the slope is shown in Figure 1, with the rows of piles installed at section A-A'. On the other hand, the details of the wedge upslope of the piles are provided in Figure 2.

The following assumptions are made when considering the upslope wedge:

1. The force  $W$  acts through the centre of the upper wedge;
2.  $\alpha_1$  is the slip surface angle with respect to the horizontal line;

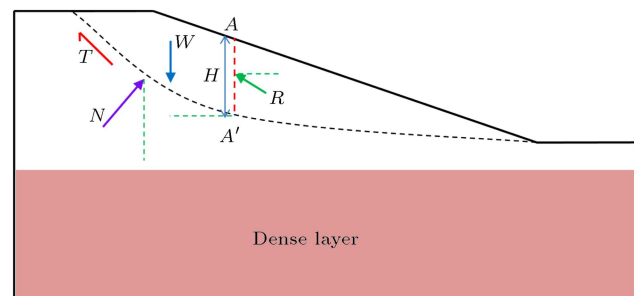


**Figure 1.** Forces on the upper wedge of the slope. Stabilizing piles are installed at section A-A'.

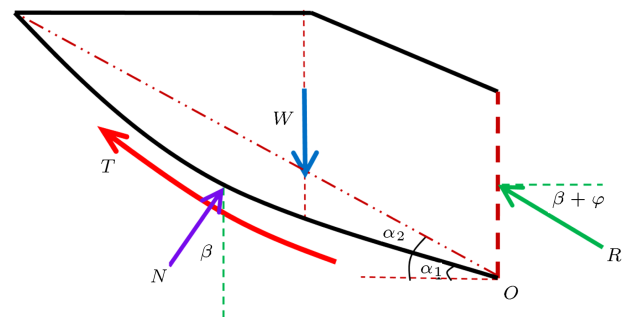


**Figure 2.** Schematic view of forces in upslope wedge.

3. The resisting force generated along the slip surface ( $T$ ) can be expressed as follows:

$$T = (C + \sigma \tan \varphi) \times L, \tag{1}$$

where  $L$  is the length of the slip surface to point O,  $C$  is the soil cohesion along the slip surface,  $\varphi$  is the friction angle, and  $\sigma$  is the average normal stress along the slip surface;

4. The force  $N$  is the normal reaction force on the slip surface; and  
 5. The angle  $\beta$  considering the whole slope is obtained from the following equation:

$$\beta = \frac{2\alpha_1 + \alpha_2}{3}, \tag{2}$$

where  $\alpha_1$  and  $\alpha_2$  are the angles as shown in Figure 2.

The reaction force,  $N$ , which is directed perpendicular to the slip surface, and the normal stress,  $\sigma$ , which develops along the slip surface, can be expressed as:

$$N = W \cos \beta, \tag{3}$$

$$\sigma = \frac{N}{L}. \tag{4}$$

Referring to the force triangle within the upper wedge as shown in Figure 3, the factor of safety of the slope against sliding,  $F_S$ , can be written as:

$$F_S = \frac{\text{Resistance force}}{\text{Driving force}}, \tag{5}$$

$$F_S = \frac{T \cos \beta + R \cos(\beta + \varphi)}{N \sin \beta}. \tag{6}$$

Substituting Eqs. (1) and (3) into Eq. (6), the force acting on the pile,  $R$ , can be determined:

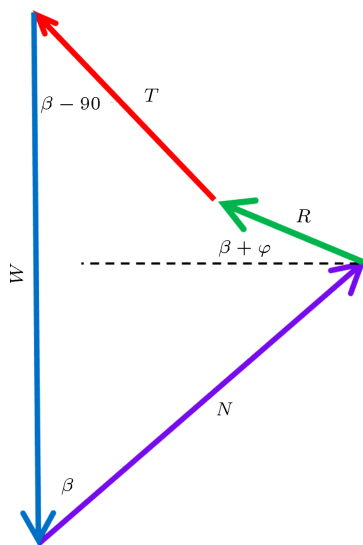


Figure 3. The force triangle in the upper wedge.

$$R = \frac{WF_S \cos \beta \sin \beta - (c + \sigma \tan \varphi) \times L \cos \beta}{\cos(\beta + \varphi)}, \tag{7}$$

$$R_{\text{shear}} = R \times \cos(\beta + \varphi) - \frac{k\gamma H^2}{2}. \tag{8}$$

In the above equations,  $\gamma$  is the unit weight of the upper soil layer,  $H$  is the length of pile above the sliding surface,  $R_{\text{shear}}$  is the total shear force on the pile just above the dense layer (see Figure 1), and the factor  $k$  depends on pile stiffness. For a flexible pile,  $k$  has a value near the coefficient of passive lateral earth pressure,  $k_p$ , while for a rigid pile, it is near the coefficient of at-rest lateral pressure,  $k_0$ . Thus, in general,  $k_0 \leq k \leq k_p$ . Note that if the downslope movement is more than the pile displacement, then there is no earth pressure acting on the pile from the downslope wedge.

A key assumption in the formulation discussed above is the expression for  $\beta$ , which is an important input into Eq. (6). From Figure 2, it is obvious that the value of  $\beta$  would range from  $\alpha_1$  to  $\alpha_2$ ; hence, it can be expressed as follows:

$$\beta = A\alpha_1 + B\alpha_2, \tag{9}$$

where  $A$  and  $B$  are coefficients which are determined by analysing hundreds of slopes and choosing the best coefficients which would provide the minimum error between numerically derived and analytically computed  $F_S$ . From such optimization procedure, Eq. (2) was initially developed; further validation of the mentioned empirical equation is discussed below.

For the purpose of validating Eq. (2), hundreds of cases of unreinforced slope were analysed using three approaches: (1) through the slope stability computer program SLOPE/W [28] to locate the critical circles; (2) using stability chart [19,20,29,30] developed based on kinematic approach of limit equilibrium analysis, such as that shown in Figure 4, where the type of failure circle is also identified; and (3) analytically using Eq. (6). Slopes with different geometries (slope angle =  $20^\circ - 45^\circ$ , slope height  $H_s = 5 - 15$  m) and different ranges of soil properties ( $4 \text{ kPa} \leq C \leq 38 \text{ kPa}$  and  $8^\circ \leq \varphi \leq 20^\circ$ ) were analysed. The entire soil slope was assumed to be dry with no water table present. For each run, the values of  $\frac{\tan \varphi}{F_S}$ ,  $\frac{C}{\gamma H_s F_S}$ , and  $\frac{C}{\gamma H_s \tan \varphi}$  were computed.

A comparison of the  $F_S$  obtained analytically using Eq. (6) and those derived using the stability chart is shown in Figure 5, while a comparison with those calculated using Bishop method in SLOPE/W is illustrated in Figure 6. Note that the proposed equation agrees very well with both the numerically calculated and chart-derived values; thus, the use of Eq. (2) to estimate  $\beta$  is well validated, at least for general homogenous slopes with  $0.5 \leq F_S \leq 2.0$ .

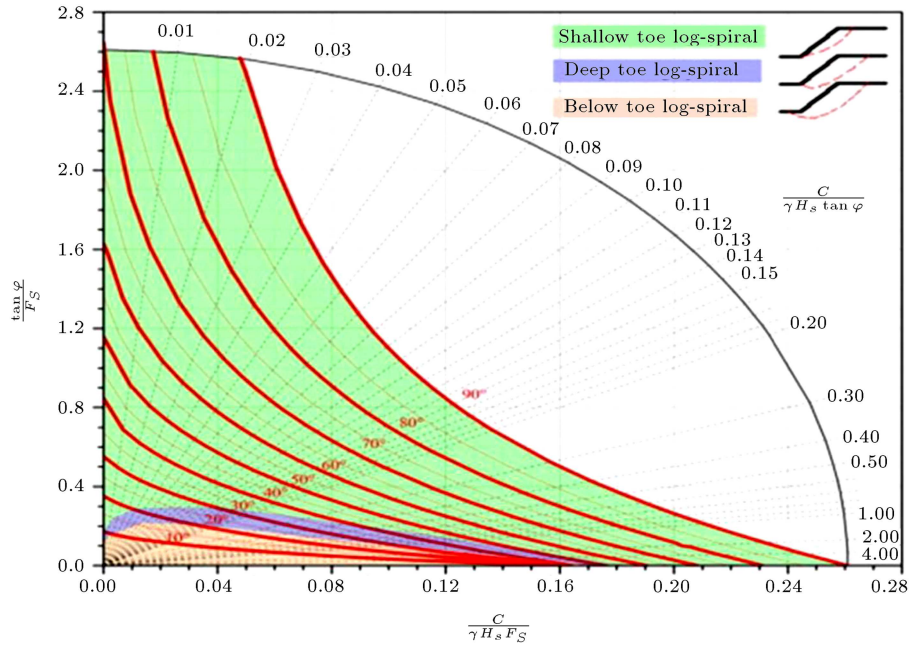


Figure 4. Proposed stability chart for  $c - \varphi$  soil [20,29,30].

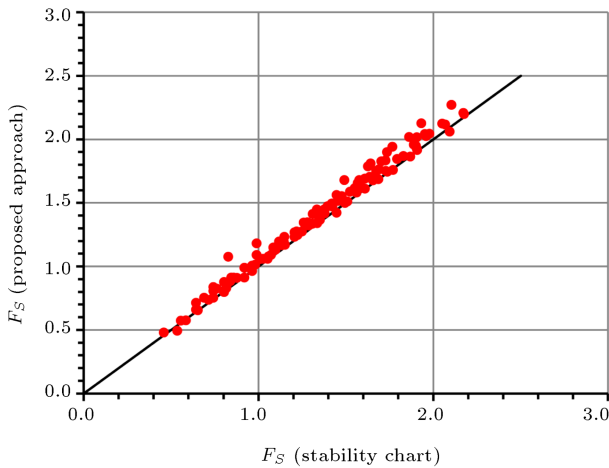


Figure 5. Comparison of factors of safety taking  $\beta$  (see Eq. (3)) with those from stability chart.

In calculating the initial factor of safety of the whole slope, it was observed that the average angle of failure wedge ( $\beta$ ) was gentler than that of a pile-reinforced slope because in the latter, the active force was due to the upslope wedge only. Thus, when analysing pile-reinforced slope, calculations indicate that instead of  $\beta$ , the average angle in the upslope wedge block is better represented by  $\beta'$ :

$$\beta' = \frac{\alpha_1 + 2\alpha_2}{3}. \tag{10}$$

Similar to Eq. (2), the above equation was obtained by analysing hundreds of reinforced slopes and determining the best expression to represent the average angle in the upslope wedge of the reinforced slope. Due to space

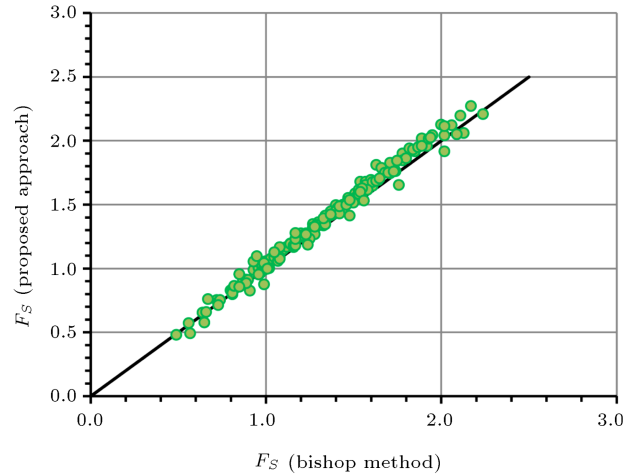


Figure 6. Comparison of factors of safety taking  $\beta$  (see Eq. (3)) with those from SLOPE/W computer program using Bishop method.

limitation, the details of the optimization process are not presented here; suffice it to say that subsequent validations presented in the latter part of the paper (through comparison with numerical methods) prove the validity of the two proposed equations.

2.2. Extension to 3-dimensional analysis

In the previous section, the magnitude of the force acting on the pile in two-dimensional case was calculated by using the wedge equilibrium method. This is now extended to three-dimension, by considering the weight of the wedge behind the piles, as indicated in Figure 7.

Focusing on the wedge behind the piles, the area of the trapezoid ( $A_1$ ) can be expressed in terms of the

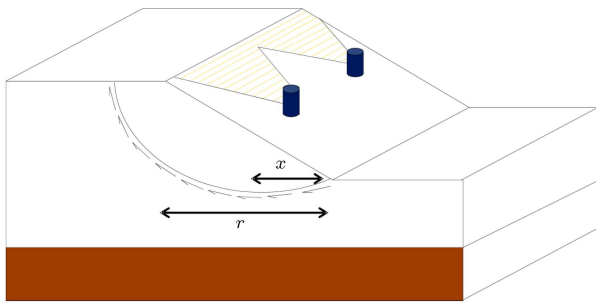


Figure 7. Schematic diagram of the slope and reinforced piles in unstable slope in 3D.

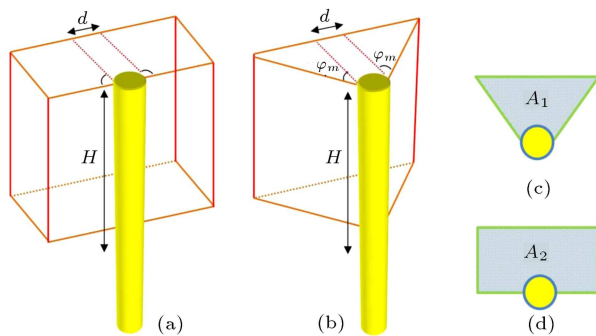


Figure 8. (a) Total area at the back of the pile. (b) Trapezoidal area and mobilized friction angle. (c)  $A_1$  area. (d)  $A_2$  area.

total area of soil at the back of the pile ( $A_2$ ) through the coefficient  $\mu$ , i.e.:

$$\mu = \frac{A_1}{A_2}. \tag{11}$$

$A_1$  and  $A_2$  are shown schematically in Figure 8. In the figure,  $\varphi_m$  is the mobilized friction angle and  $d$  is the diameter of the pile.

To calculate the areas  $A_1$  and  $A_2$ , it is required to calculate the base length of the trapezoid, denoted by  $BC$  in Figure 9. In the proposed approach,  $BC$  is calculated based on the equation developed by Ashour and Ardalan [1]; however, instead of  $BC$  varying with depth as originally proposed, the current formulation assumes that it is constant with depth.

In addition, the magnitude of  $BC$  depends on the mobilized friction angle ( $\varphi_m$ ) of the soil behind the piles, which is a function of strain, depth, and stress within the soil. Considering the stress-strain behaviour of the soil as shown in Figure 10, the additional horizontal stress,  $\Delta\sigma_h$ , can be expressed as:

$$\Delta\sigma_h = SL \times \Delta\sigma_{hf}, \tag{12}$$

where  $SL$  (Stress Level) is the ratio of the additional horizontal stress at any depth to the additional horizontal stress at failure mode. As shown in Figure 10,  $SL$  increases with increase in strain, indicating that

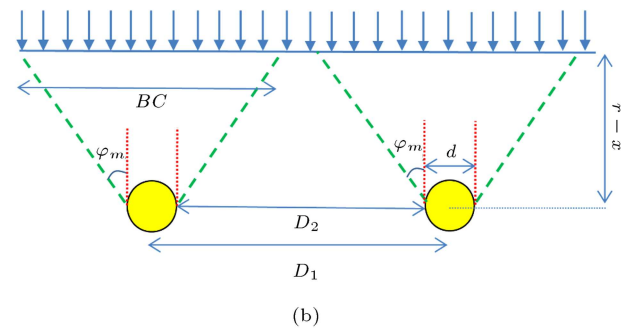
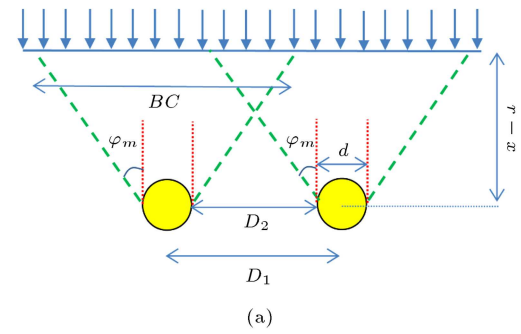


Figure 9. Different states of soil mass behind the pile.

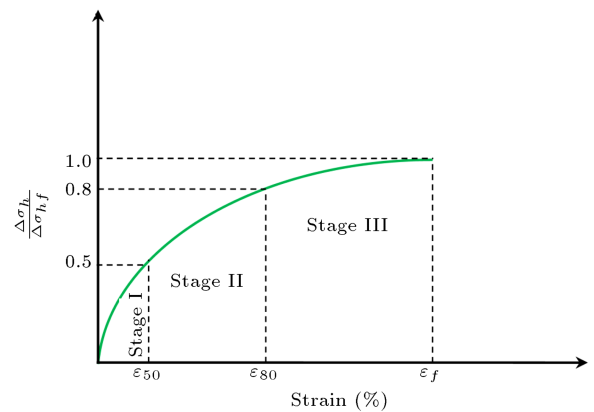


Figure 10. Soil stress-strain relationship (adopted from [1]).

with any increase the horizontal stress moves closer to the failure stress; thus, the diameter of the Mohr circle and the magnitude of  $\varphi_m$  increase.

This is depicted in Figure 11, where it is observed that in all states,  $\varphi_m$  value is lower than the  $\varphi$  value (soil friction angle) as determined from Eq. (13):

$$\tan \varphi_m = \frac{\tan \varphi}{F_{S_0}}, \tag{13}$$

where  $F_{S_0}$  is initial safety factor of slope. Therefore, from Figure 9, it follows that:

$$BC = d + 2(r - x) \tan \varphi_m. \tag{14}$$

Going back to Eq. (11), there are two cases to calculate  $\mu$ :

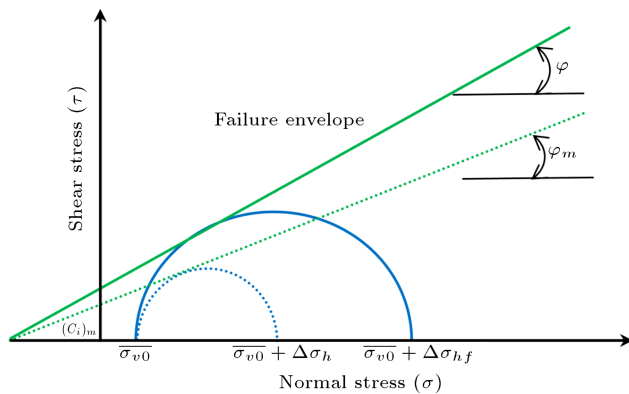


**Figure 11.** Mobilized effective friction angle with the change in soil stress.

- **Case (a):**  $D_2 < BC - d$  (refer to Figure 9(a)):

$$A_1 = A_2 - \frac{D_2^2}{4 \tan \varphi_m}, \quad (15a)$$

$$A_2 = (r - x) \times (d + D_2), \quad (15b)$$

$$\mu = \frac{A_2 - \frac{D_2^2}{4 \tan \varphi_m}}{A_2} = 1 - \frac{D_2^2}{4A_2 \tan \varphi_m}. \quad (15c)$$

- **Case (b):**  $D_2 > BC - d$  (refer to Figure 9(b)):

$$A_1 = \frac{BC \times (r - x)}{2}, \quad (16a)$$

$$A_2 = (r - x) \times (d + D_2), \quad (16b)$$

$$\mu = \frac{\frac{BC \times (r - x)}{2}}{(r - x) \times (d + D_2)} = \frac{BC}{2(d + D_2)}. \quad (16c)$$

Therefore, the force acting on the piles (in 3-D state) can be expressed as a function of the weight of wedge behind the piles, soil properties (friction angle, cohesion), sliding geometry (upstream slide surface length, the mean of the depth of upper wedge, sliding angle), distance between piles, pile diameter, and coefficient  $\mu$ , i.e.:

$$R_{(\text{shear-3D})} = \mu \times R_{\text{shear}} \times (D_2 + d). \quad (17)$$

In calculating the factor of safety of slopes stabilized by piles, Eq. (6) is used together with the allowable shear resistance of the pile and the effect of pile spacing, i.e.:

$$F_S = \frac{P_{\text{pile}}}{\mu \times (D_2 + d)} + \frac{(c + \sigma \tan \varphi) \times L}{W \sin \beta}$$

$$D_2 < BC - d, \quad (18a)$$

$$F_S = \frac{P_{\text{pile}}(BC - d)}{\mu \times (D_2 + d)} + \frac{(c + \sigma \tan \varphi) \times L}{W \sin \beta}$$

$$D_2 > BC - d, \quad (18b)$$

In the above equations,  $P_{\text{pile}}$  is the extra force due to the reinforcement with pile, which can be expressed as:

$$P_{\text{pile}} = \frac{V_{\text{max}} \pi H d^2}{8} + \frac{k \gamma H^2}{2}, \quad (19)$$

where  $V_{\text{max}}$  is the allowable maximum shear stress;  $H$  is the length of pile within the slip wedge; and  $D_2$  is the clear spacing between piles.

### 2.3. Arching effect

One of the main mechanisms in enhancing the stability of the soil slope through piles is soil arching, which is the transfer of soil stresses from a yielding mass of soil on to adjacent stationary parts. Engineering practices and laboratory experiments have shown that single piles, such as piles embedded into a firm, non-yielding base in a slope, can provide significant additional stability to the slope if conditions for soil arching are met [22].

One important consideration in the design of piles in stabilizing slopes is the maximum allowable spacing between the piles so that soil arching is still maintained. Practical recommendations have been obtained from laboratory studies. For example, Chen & Poulos [4] conducted a series of laboratory tests on the group effects of piles subjected to soil movement, where the effects of free head and capped head were investigated. Test results indicated that when the pile spacing was equal to or larger than eight times the pile diameter, the piles in the group behaved as if they were individual piles. Similar results regarding the critical ratio of clear spacing to pile diameter were also found in the arching model test conducted by Adachi et al. [31].

In the present study, arching effect is introduced in the proposed procedure through the coefficient  $\mu$ , given by Eq. (11). Overlapping of the wedges behind the piles, as illustrated in Figure 9(a), shows arching effect in the analysis. The arching phenomenon between piles is also examined numerically using the computer software PLAXIS 2D [32]. The soil parameters used are as follows:  $E = 12$  MPa,  $C = 10$  kPa, and  $\varphi = 15^\circ$ . The clear spacing between the piles varies between 1-6 times the pile diameter ( $d = 1$  m) and its effect on the occurrence of arching is examined. Figure 12 shows the displacement contours under large ground deformation where it is obvious that at large spacing, the soil practically moves around the pile; on the other hand, arching is very effective at small pile spacing. Note that in addition to pile spacing, soil parameters are also very important in inducing arching effect.

Based on Figure 12 and supported by other research results [4,22,31,33-35], pile spacing less than five times the pile diameter is required to generate group effect and the associated soil arching between the piles. For pile spacing greater than five times the pile diameter, the piles behave almost as single

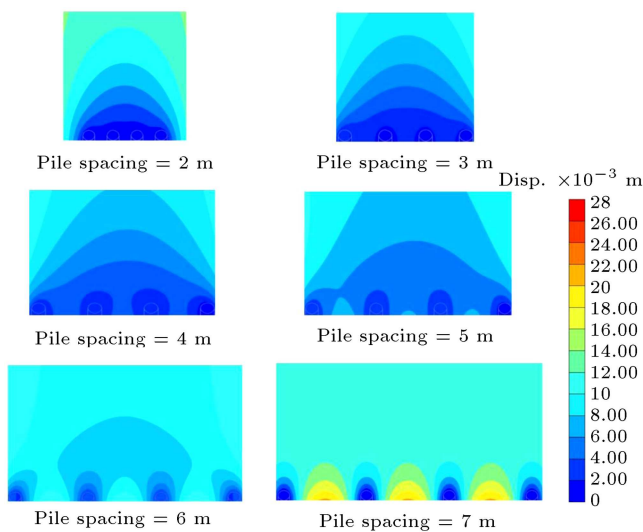


**Figure 12.** Effect of variation of pile spacing on arching ( $C = 10$  kPa,  $\varphi = 15^\circ$ ).

individual piles and the soil can flow around them. Hence, large pile spacing is not recommended for slope stabilization and therefore, further examination is not required. Pile spacing of four times the pile diameter is believed to be the most cost-effective arrangement for pile rows, because it provides the optimum spacing (i.e., the minimum number of piles) required to produce soil arching between the piles for the inter-pile soil to be adequately retained. This arrangement is often adopted in engineering practice as the optimal pile spacing in slope stabilization applications [33].

### 3. Verification

#### 3.1. Comparison with model experiments

A series of physical model tests was conducted on reinforced slopes with a 1/10 scale. The sandy model slope was placed on a box measuring 2.5 m  $\times$  1.5 m  $\times$  1.5 m. Prior to construction of the model slope, silty sand was first placed inside the box and compacted under different degrees of compaction. For each degree of compaction, the soil properties were measured by performing element tests. Based on the results, a suitable condition for the physical tests was selected. The relevant soil parameters were:  $\gamma = 19$  kN/m<sup>3</sup>,  $C = 1$  kPa, and  $\varphi = 20^\circ$ . In the all the tests involving reinforced pile models, hollow plastic pipes, with outer diameter of 150 mm and thickness of 4 mm, were driven at the middle of the slope with various spacing and embedded at least 20 cm into the stiff base layer (consisting of polystyrene layer). Figure 13 shows the model slope reinforced by piles. Markers at 10 cm interval were placed on the side of the slope and their movements were tracked by a camera at regular intervals. The piles were not instrumented.

The initial factor of safety ( $F_S$ ) of the unrein-

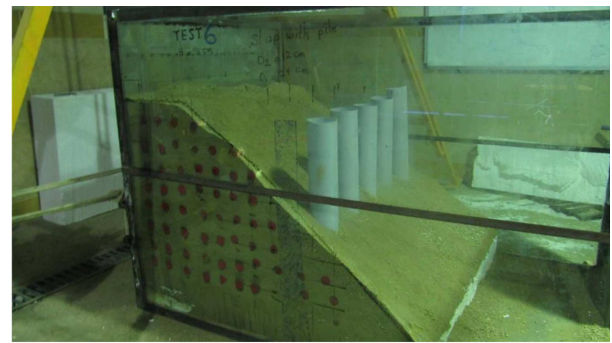


**Figure 13.** Physical model test of stabilized slope.

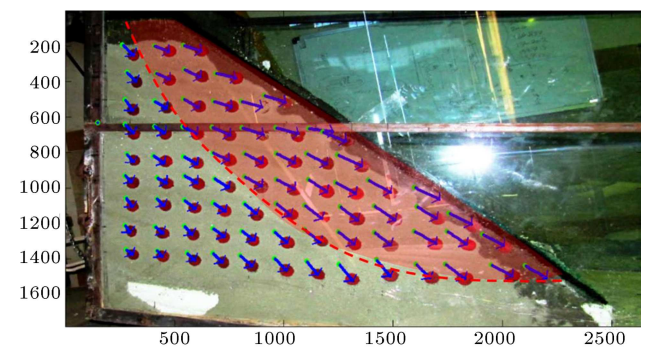


**Figure 14.** Displacement vectors in the unreinforced slope at inclination angle of  $8^\circ$ .

forced slope was calculated to be  $F_S = 1.29$  using the computer program SLOPE/W. In order to induce instability, the slope angle should be increased; for this purpose, one side of the box was slowly raised using a crane such that the base would be inclined at various angles, up to  $10^\circ$ . During the tests, the movements of the markers were tracked and then processed to determine the displacement vectors.

Figure 14 shows the state of the unreinforced slope at an inclination angle of  $8^\circ$ . It is clear that at this state, the slope became unstable and movement was initiated. The displacement vectors show a very clear sliding wedge, as indicated in the figure.

For this unreinforced slope, a comparison is made between the  $F_S$  at various inclination angles calculated using SLOPE/W and those calculated using the proposed analytical approach and the results are summarised in Table 1. Good agreement can be observed between the results from the proposed method and those observed from the model tests. Note that when the inclination angle was  $8^\circ$ , the parameters used in Eq. (6) were:  $\alpha_1 = 30^\circ$ ,  $\alpha_2 = 46^\circ$ ,  $L = 2.2$  m, and  $W = 12.7$  kN/m.

It is worthy to mention that progressive failure was not observed in the model test. The small displacements observed when the inclination angle was  $4\text{--}6^\circ$  were surficial in nature and did not represent progressive movement. However, when the inclination angle was  $8^\circ$ , failure was mobilized and the slope began

**Table 1.** Comparison between factors of safety computed using SLOPE/W and the proposed method for unreinforced slope with different inclination angles.

Inclination angle (°)	$F_S$ (numerical)	$F_S$ (analytical)	Comments
0	1.29	1.35	Slope is stable
2	1.22	1.26	Slope is stable
4	1.13	1.18	Stable, with small displacement
6	1.07	1.09	Stable, with small displacement
8	0.89	0.96	Slope begins to move

to move, consistent with the prediction of the numerical model.

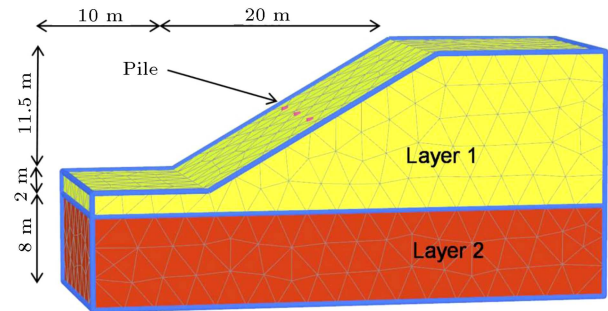
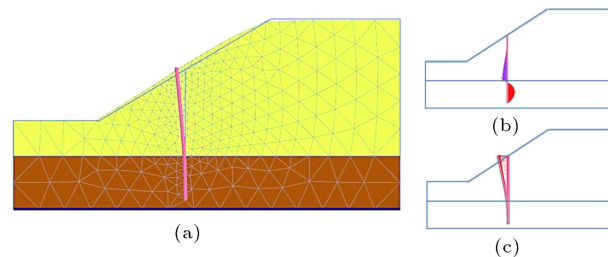
Model tests were also done on reinforced slopes with various spacing between piles, i.e.,  $1D$ ,  $2D$ ,  $3D$ , and  $4D$ , where  $D$  is the pile diameter. Similar to the unreinforced slope, the box was tilted to induce movement of the slope and the resulting ground deformation was tracked for various inclination angles. Again, the factor of safety calculated numerically (using FLAC3D) was compared with those obtained using the proposed approach. Table 2 summarises the results of the comparison for the case with pile spacing corresponding to  $4D$ ; it is obvious from the table that a good agreement exists between the two methods.

It is unfortunate that the piles were not instrumented and the actual forces on the piles cannot be compared with those calculated using the proposed method. Nevertheless, the applicability of the proposed method is shown by the good agreement between the  $F_S$  obtained analytically and using the proposed method for different inclination angles.

### 3.2. Comparison with numerical approach

As another example to verify the applicability of the proposed approach, a soil slope with the height of  $H_s = 11.5$  meters and slope angle of  $30^\circ$  is analysed and the results are compared with those obtained using PLAXIS 3D [36] and other equations in the literature. The slope is described in Figures 15 and 16 while the soil and pile properties are summarised in Table 3.

At this stage, the force acting on the stabilizing piles is calculated using three different methods: (1) Ito and Matsui method [21]; (2) numerical analysis using PLAXIS 3D; and (3) the proposed analytical

**Figure 15.** Finite element mesh for slope (slope angle =  $30^\circ$ ,  $H_s = 11.5$  m).**Figure 16.** (a) Deformed slope (slope angle =  $30^\circ$  and  $H_s = 11.5$  m). (b) Shear force distribution on pile. (c) Pile displacement.

approach. For the third method, the sliding wedge can be divided into two parts, namely, upslope and downslope, after which the force acting on the piles is calculated using the upslope wedge equilibrium (using the data in Table 3). In calculating the force acting on the piles according to Eq. (17), the essential parameters could be calculated based on upstream wedge of the slope (Figure 9). These parameters are shown in

**Table 2.** Comparison between factors of safety computed using FLAC3D and the proposed method for reinforced slope (pile spacing =  $4D$ ) with different inclination angles.

Inclination angle (°)	$F_S$ (numerical)	$F_S$ (analytical)	Comments
0	1.61	1.55	Stable
3	1.51	1.42	Stable
7	1.36	1.27	Stable
10	1.25	1.19	Stable
13	1.13	1.08	Stable
16	0.98	0.94	Sliding

**Table 3.** Input parameters used in analysing pile-stabilized slope.

	Layer 1	Layer 2	Pile
Model	Mohr-Coulomb		Elastic
Unit weight (kN/m <sup>3</sup> )	18		23
Cohesion (kPa)	10	Stiff zone	–
Friction angle (°)	15		–
Elastic modulus (MPa)	12		23000
Poisson’s ratio	0.3		0.25

**Table 4.** Essential parameters for calculating the force acting on the pile using the proposed approach.

$D_2$	$d$	Case	$A_1$	$A_2$	$\mu$
1	1	a	18.8	20	0.94
2	1	a	25.2	30	0.84
3	1	a	29.4	40	0.73
4	1	a	31.2	50	0.62
5	1	b	26.3	60	0.48
6	1	b	26.3	70	0.37

Note: For definition of “Case”, please refer to Figure 9.

Table 4. Note that in the table, Cases (a) and (b) are illustrated in Figures 9(a) and 9(b), respectively.

Once the required parameters have been determined as in Table 4, the force acting on the pile could be found using the above formulations. The results are summarized in Table 5 and plotted in Figure 17. As shown in the figure, the shear force on the pile increases with increase in pile spacing until arching occurs between piles at spacing of around 6 times the pile diameter. Beyond that, the shear force on the pile becomes more or less constant, indicating that they are acting as discrete individual piles.

The results are compared with those obtained numerically using PLAXIS 3D, where a good correlation is observed as shown in Figure 17. The results for both the analytical approach and the numerical method are opposite to that obtained from Ito and Matsui equation, which is valid only over a limited range of spacing; at large spacing or at very close spacing, the

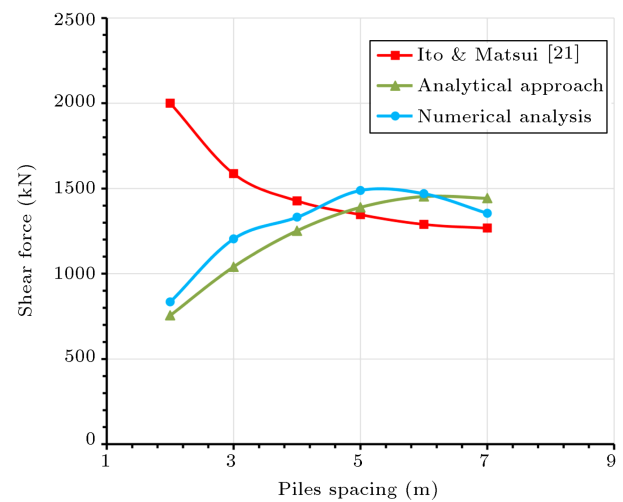


**Figure 17.** Computed force acting on pile for various pile spacing.

mechanism of flow through the piles postulated by Ito and Matsui [21] is not the critical mode [37].

Based on PLAXIS3D numerical analysis, the shear force and bending moment at any point within the pile could be calculated and their variations with depth for various pile spacings are shown in Figures 18 and 19, respectively. As seen in Figure 18, with increase in the pile spacing, the shear force developing on the piles increases until arching occurs between piles.

For practical purposes, the determination of the target factor of safety ( $F_S$ ) after stabilization is important. Using Eqs. (18a) and (18b) for various allowable shear stresses on the pile, the factors of safety for various pile spacings are calculated and plotted in

**Table 5.** Shear forces on pile for various pile spacings based on the proposed approach.

Pile spacing (m)	$D_2$ (m)	$d$ (m)	Weight of wedge (kN/m)	$\mu$	Shear force on pile (kN)
2	1	1	1335	0.94	755
3	2	1	1335	0.84	1040
4	3	1	1335	0.73	1252
5	4	1	1335	0.62	1389
6	5	1	1335	0.48	1452
7	6	1	1335	0.37	1442

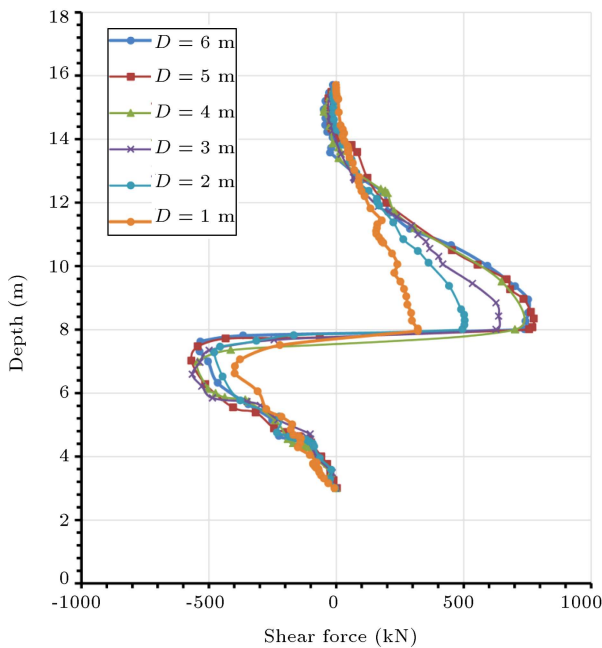


Figure 18. Shear force on pile for various pile spacings.

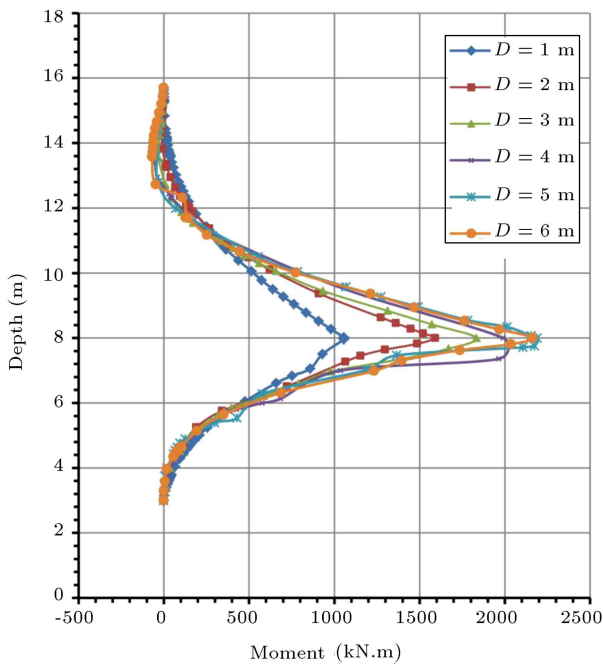


Figure 19. Bending moment on pile for various pile spacings.

Figure 20. As expected,  $F_S$  decreases as the pile spacing increases. From the figure, the values obtained analytically are in agreement with those obtained numerically using PLAXIS 3D.

#### 4. Conclusions

An analytical approach was proposed to analyse the stability of slopes reinforced by piles by considering

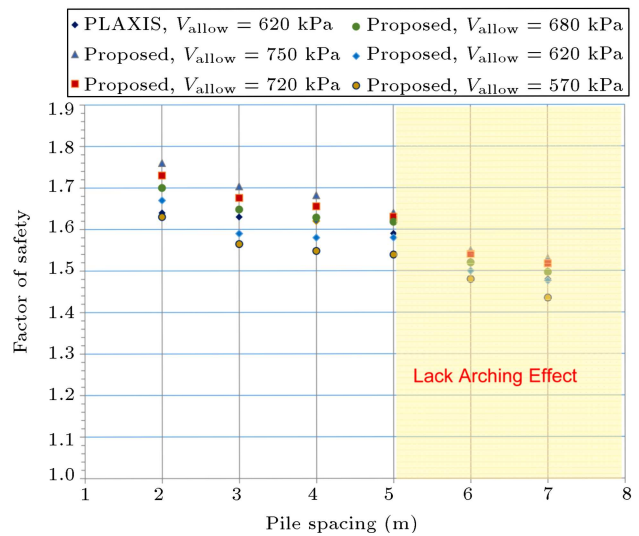


Figure 20. Comparison of factors of safety of a slope with various pile spacings computed analytically and numerically.

limit equilibrium of the sliding wedge upslope of the pile. The following are the major conclusions obtained:

- Once the initial sliding surface is determined, say using some simple slope stability algorithms, site investigation, or simple software, the factor of safety of both reinforced and unreinforced slopes as well as the acting forces on the stabilizing piles can be determined;
- Using the proposed method, analyses showed that the force acting on the stabilizing pile decreased when pile spacing exceeded more than five times the pile diameter because at this spacing, the piles behaved almost as single isolated piles and the soil could flow between them. Hence, such an arrangement cannot be recommended for the purpose of slope stabilization;
- The proposed analytical method calculated factors of safety, which were in agreement with the results of laboratory model tests and numerical analyses;
- The forces on the pile calculated using the proposed analytical method also agreed quite well with the results of numerical analysis. Compared with those obtained from Ito and Matsui equation, the results are comparable, except at very closed pile spacing where the latter equation is not applicable due to a different mechanism assume;
- Because of its simplicity and ease of use, it can be very useful in practical applications.

#### Acknowledgment

The main part of this research was undertaken when the second author was a visiting researcher at the

University of Auckland. His visit was made possible through the financial support provided by the Ministry of Science, Research and Technology of Iran and this is gratefully acknowledged.

## References

- Ashour, M. and Ardalan, H. "Analysis of pile stabilized slopes based on soil-pile interaction", *Computers and Geotechnics*, **39**, pp. 85-97 (2012).
- Ito, T., Matsui, T., and Hong, P.W. "Design method for stabilizing piles against landslide - one row of piles", *Soils and Foundations*, **21**(1), pp. 21-37 (1981).
- Poulos, H.G. "Design of reinforcing piles to increase slope stability", *Can. Geotech. J.*, **32**(5), pp. 808-818 (1995).
- Chen, L.T. and Poulos, H.G. "Piles subjected to lateral soil movements", *J. Geotech. Geoenviron Eng. ASCE*, **123**(9), pp. 802-811 (1997).
- Zeng, S. and Liang, R. "Stability analysis of drilled shafts reinforced slope", *Soils and Foundations*, **42**(2), pp. 93-102 (2002).
- Won, J., You, K., Jeong, S., and Kim, S. "Coupled effects in stability analysis of pile-slope systems", *Computers and Geotechnics*, **32**(4), pp. 304-315 (2005).
- Wei, W.B. and Cheng, Y.M. "Strength reduction analysis for slope reinforced with one row of piles", *Computers and Geotechnics*, **36**(7), pp. 1176-1185 (2009).
- Kourkoulis, R. and Gelagoti, F. "Slope stabilizing piles and pile-groups: parametric study and design insights", *J. Geotech. Geoenviron. Eng., ASCE*, **137**(7), pp. 663-677 (2011).
- Alkasawneh, W., Malkawi, A.H., Nusairat, J.H., and Albataineh, N. "A comparative study of various commercially available programs in slope stability analysis", *Computers and Geotechnics*, **35**, pp. 428-435 (2008).
- Hassiotis, S., Chameau, J.L., and Gunaratne, M. "Design method for stabilization of slopes with piles", *J. Geotech. Geoenviron. Eng., ASCE*, **123**(4), pp. 314-323 (1997).
- Huang, C.C., Tsai, C.C., and Chen, Y.H. "Generalized method for three-dimensional slope stability analysis", *J. Geotech. Geoenviron Eng, ASCE*, **128**(10), pp. 836-848 (2002).
- Huang, M., Wang, H., Sheng, D., and Liu, Y. "Rotational-translational mechanism for the upper bound stability analysis of slopes with weak inter-layer", *Computers and Geotechnics*, **53**, pp. 133-141 (2013).
- Chen, W.F. "Limit analysis and soil plasticity", *Elsevier Scientific Publishing Company*, New York (1975).
- Hajiazizi, M. and Tavana, H. "Determining three-dimensional non-spherical critical slip surface in earth slopes using an optimization method", *Engineering Geology*, **153**, pp. 114-124 (2013).
- Ausilio, E., Conte, E., and Dente, G. "Stability analysis of slopes reinforced with piles", *Computers and Geotechnics*, **28**, pp. 591-611 (2001).
- Nian, T.K., Chen, G.Q., Luan, M.T., Yang, Q., and Zheng, D.F. "Limit analysis of the stability of slopes reinforced with piles against landslide in non-homogeneous and anisotropic soil", *Canadian Geotechnical Journal*, **45**(8), pp. 1092-1103 (2008).
- Liang, R.Y., Joorabchi, A.E., and Li, L. "Design method for drilled shaft stabilization of unstable slopes", *Geo-Congress 2013, ASCE*, pp. 2024-2033 (2013).
- Cai, F. and Ugai, K. "Numerical analysis of the stability of a slope reinforced with piles", *Soils and Foundations*, **40**, pp. 73-84 (2000).
- Michalowski, R.L. "Stability charts for uniform slopes", *J. Geotech Geoenviron Eng, ASCE*, **128**(4), pp. 351-355 (2002).
- Tang, G., Zhao, L., Li, L., and Yang, F. "Stability charts of slopes under typical conditions developed by upper bound limit analysis", *Computers and Geotechnics*, **65**, pp. 233-240 (2015).
- Ito, T. and Matsui, T. "Methods to estimate lateral force acting on stabilizing piles", *Soils and Foundations*, **15**(4), pp. 43-59 (1975).
- Kourkoulis, R., Gelagoti, F., Anastasopoulos, L., and Gazetas, G. "Hybrid method for analysis and design of slope stabilizing piles", *Journal of Geotechnical and Geoenvironmental Engineering, ASCE*, **138**(1), pp. 1-14 (2012).
- Liang, R.Y. and Yamin, M.M. "Three dimensional finite element study of arching behavior in slope/drilled shafts system", *Int J Numer Anal Methods Geomech*, **34**(11), pp. 1157-1168 (2010).
- Lee, C.Y., Hull, T.S., and Poulos, H.G. "Simplified pile-slope stability analysis", *Computers and Geotechnics*, **17**(1), pp. 1-16 (1995).
- Li, X., He, S., and Wu, Y. "Seismic displacement of slopes reinforced with piles", *Journal of Geotechnical and Geoenvironmental Engineering, ASCE*, **136**(6), pp. 880-884 (2010).
- Broms, B. "Lateral resistance of piles in cohesionless soils", *J. Soil Mech. Found. Div*, **90**(3), pp. 123-156 (1964).
- Kahyaoglu, M., Onal, O., and Imançlı, G. "Soil arching and load transfer mechanism for slope stabilized with piles", *Journal of Civil Engineering and Management*, **18**(5), pp. 701-708 (2012).
- GEO-SLOPE International Ltd. *Stability Modeling with SLOPE/W 2007: An Engineering Methodology*, 4th Ed. Alberta, Canada (2015).
- Steward, T., Sivakugan, N., Shukla, S.K., and Das, B.M. "Taylor's slope stability charts revisited", *Int J Geomech*, **11**(4), pp. 348-52 (2011).

30. Hajiazizi, M. and Mazaheri, A.H. “The use of the line segments slip surface for location optimization of pile in stabilization of earth slopes”, *International Journal of Civil Engineering*, **13**(1), pp. 14-27 (2015).
31. Adachi, T., Kimura, M., and Tada, S. “Analysis on the preventive mechanism of landslide stabilizing piles”, *Numerical Models in Geomechanics (NUMOG III)*, Elsevier, pp. 691-698 (1989).
32. Plaxis. *PLAXIS 2D Reference Manual*. Delft, Netherlands (2015).
33. Boshcher, P.J. and Gray, D.H. “Soil arching in sandy slopes”, *J. Geotech. Engrg., ASCE*, **112**(6), pp. 626-645 (1986).
34. Smethurst, J.A. and Powrie, W. “Monitoring and analysis of the bending behaviour of discrete piles used to stabilise a railway embankment”, *Géotechnique*, **57**(8), pp. 663-677 (2007).
35. Liang, R. and Zeng, S. “Numerical study of soil arching mechanism in drilled shafts for slope stabilization”, *Soils and Foundations*, **42**(2), pp. 83-92 (2002).
36. Plaxis. *PLAXIS 3D Reference Manual*, Delft, Netherlands (2015).
37. Poulos, H.G. “Design of slope stabilizing piles”, *Slope Stability Engineering*, J.C. Jiang, N. Yagi, and T. Yamagami, Eds., Balkema, Rotterdam, Netherlands (1999).

## Biographies

**Mohammad Hajiazizi** is an Associate Professor of Geotechnical Engineering at Razi University, Kermanshah. He received his PhD degree in Geotechnical Engineering from Shiraz University in Iran, and his MSc degree in Geotechnical Engineering from Tarbiat Modares University. His current and main research interests are soil improvement, slope stability, tunnelling, and meshless methods.

**Ahmad Reza Mazaheri** is an Assistant Professor of Geotechnical Engineering at University of Ayatollah ozma Boroujerdi. He received his PhD degree in Geotechnical Engineering from Razi University and his MSc degree in Geotechnical Engineering from Amirkabir University of Technology. His current and main research interests are slope stability and soil improvement.

**Rolando P. Orense** is an Associate Professor at the University of Auckland, New Zealand. He received his DEng degree from the University of Tokyo, Japan. His research interests are geotechnical earthquake engineering/soil dynamics, soil liquefaction and ground remediation techniques, slope movements and landslide risk mitigation, and site and soil characterization.